



LAWRENCE
LIVERMORE
NATIONAL
LABORATORY

Unforced, Forced and Resonance-Forced Waves in a Spherical Atmosphere

C. Covey

October 27, 2015

Disclaimer

This document was prepared as an account of work sponsored by an agency of the United States government. Neither the United States government nor Lawrence Livermore National Security, LLC, nor any of their employees makes any warranty, expressed or implied, or assumes any legal liability or responsibility for the accuracy, completeness, or usefulness of any information, apparatus, product, or process disclosed, or represents that its use would not infringe privately owned rights. Reference herein to any specific commercial product, process, or service by trade name, trademark, manufacturer, or otherwise does not necessarily constitute or imply its endorsement, recommendation, or favoring by the United States government or Lawrence Livermore National Security, LLC. The views and opinions of authors expressed herein do not necessarily state or reflect those of the United States government or Lawrence Livermore National Security, LLC, and shall not be used for advertising or product endorsement purposes.

This work performed under the auspices of the U.S. Department of Energy by Lawrence Livermore National Laboratory under Contract DE-AC52-07NA27344.

Unforced, Forced and Resonance-Forced Waves in a Spherical Atmosphere

This technical report discusses a longstanding issue of atmospheric tides in weather-prediction and general circulation models (GCMs). Tidal signatures consistent with observations have appeared in the surface pressure output of GCMs since their inception (Hardy 1968, Hunt and Manabe 1968). Such models, however, are sufficiently complicated that the possibility of “getting the right answer for the wrong reasons” arises. Lindzen et al. (1968, hereafter LBK) showed that wave reflection at the upper boundary of a GCM can artificially enhance the tides. Covey et al. (2011, 2014) found that tidal output from a number of modern GCMs is surprisingly independent of their forcing. This finding is consistent with earlier suggestions that a compensating effect occurs in some models: lowering the model top reduces the forcing (solar heating of the ozone layer) but also enhances spurious wave reflection (Zwiers and Hamilton 1986, Hamilton et al. 2008).

The linear calculations below assess the possibility of this compensating effect in modern GCMs, given modern upper boundary conditions. I follow classical tidal theory (Chapman and Lindzen 1970) with modern notation (Forbes 1995), first recapitulating LBK’s main points, then briefly considering how they might apply to modern GCMs.

Classical theory of unforced waves

First, linearize the equations of motion about an isothermal and motionless background state with perturbations proportional to $e^{i(s\lambda - \sigma t)}$ where $s = 1, 2, 3, \dots$, $\lambda =$ longitude and t is time. Eliminating variables gives a single second-order partial differential equations in one variable; the conventional choice is geopotential height perturbation Φ as a function of latitude φ and altitude z^* . Due to the symmetry of the background state, the equation is separable. Writing

$$\Phi(\varphi, z^*) = \Theta(\varphi) G(z^*) e^{z^*/2H} \quad (*1*)$$

and introducing a separation constant h gives two ordinary differential equations:

$$L_{s,\sigma}[\Theta] + \frac{(2\Omega a)^2}{gh} \Theta = 0 \quad (*2*)$$

[= Eq. (4) in LBK]

$$\frac{d^2 G}{dz^{*2}} - \left(\frac{1}{4} - \frac{\kappa H}{h}\right) G \equiv \frac{d^2 G}{dz^{*2}} - \mu^2 G = [\text{heating}] \quad (*3*)$$

[= Eq. (7) in LBK]

In these equations, Ω and a are planetary rotation rate and radius respectively, $\kappa = R / c_p$ ($\approx 2/7$ for diatomic molecules, but from basic thermodynamics always $< 2/5$), and the scale height H is proportional to the assumed constant background temperature. The operator $L_{s,\sigma}$ involves derivatives with

respect to φ . It is called Laplace's tidal operator and Eq. (2) is called Laplace's tidal equation. Waves in a global ocean of depth h obey Laplace's tidal equation, but here h is just a separation constant. Eq. (3) is called the vertical structure equation. Here $x \equiv z^*/H$, the approximate altitude in scale heights, but z^* cannot be physical altitude if geopotential height is already a dependent variable. To be precise, $z^* \equiv H \log(p/p_s)$ where p_s is the *constant global mean* of surface pressure (as in Holton 1975, Section 2.4.1).

Free oscillations (normal modes) occur when the solar heating term Eq. (3) vanishes; in this case its general solution is:

$$\mathbf{G}[\mathbf{x}_-] := \mathbf{e}^{-\mu \mathbf{x}} + \mathbf{A} \mathbf{e}^{+\mu \mathbf{x}}; \quad (*4*)$$

Since $L_{s,\sigma}$ is a self-adjoint (Hermitian) operator, its eigenvalues are all real; hence μ^2 is real and μ is either real or pure imaginary. Without loss of generality, define μ as the positive or positive-imaginary square root (depending on the sign of μ^2) so that A in Eq. (4) is the coefficient of the positive or positive-imaginary exponential.

Normal modes exist at particular values of μ (eigenvalues) that allow $G(x)$ to satisfy appropriate boundary conditions. Note from Eq. (3) that determining μ is equivalent to determining h/H . Therefore, after solving the vertical structure equation (3) to get a separation constant h , one may solve Laplace's tidal equation as a second eigenvalue problem: given a value of $gh/(2\Omega a)^2$, each choice of zonal wavenumber s generates a series of normal-mode frequencies σ (Longuet-Higgins 1968).

For an atmosphere, the lower boundary condition on Eq. (3) is that physical vertical velocity (*not* the pressure-coordinate vertical velocity $w^* \equiv dz^*/dt$) vanish. Linearizing this condition gives a homogeneous equation relating Φ and w^* at $z^* = 0$. In the unforced case, a second homogeneous equation relating Φ and w^* is provided by the thermodynamic energy equation: $w^* \propto \partial\Phi/\partial z^* \propto \partial(Ge^{z^*/2H})/\partial z^*$.

Eliminating w^* , the end result (Holton 1975, Section 2.4.1) is $\frac{dG}{dx} + (\frac{1}{2} - \kappa)G = 0$ at $x = 0$. The same result may be deduced from Chapter 9 of Lindzen (2005; note he prefers to eliminate Φ rather than w^*).

Substituting the functional form of $G(x)$ from Eq. (4) then determines A as a function of μ and κ :

$$\mathbf{A} \rightarrow \frac{1 - 2\kappa - 2\mu}{-1 + 2\kappa - 2\mu}$$

(*5*)

The next step is to apply the upper boundary condition, which depends on whether the atmosphere is bounded or unbounded in the vertical dimension.

(a) Unbounded atmospheres

If the atmosphere extends infinitely upward, the upper boundary condition for normal modes is that energy per unit volume decrease with height. Recalling the factor $e^{z^*/2H}$ in Eq. (1) and noting that energy per unit mass $\propto \Phi^2$ while mass per unit volume $\propto e^{-z^*/H}$, it follows that the upper boundary condition requires that $\|G\|$ decrease with height. Thus $\mu^2 > 0$ and $A = 0$ in Eq. (4). (A radiation boundary condition -- in which $\mu^2 < 0$ and the sign of $\text{Im}(\mu)$ is chosen to make energy propagation upward at the top boundary -- is unphysical in the absence of forcing.) Eq. (5) then implies $\mu = \frac{1}{2} - \kappa$, or in terms of h :

$$h \rightarrow \frac{H}{1 - \kappa}$$

(*6*)

This condition on h is identical to Eq. (20) in Forbes (1995) and is consistent with the lower boundary condition given by Eq. (8) in LBK.

Note that only one equivalent depth exists for normal modes of an unbounded isothermal atmosphere. (If the background atmospheric temperature varied in height, an additional term dH/dx would appear in the expression for μ^2 in Eq. (3) and additional h values could exist.) Taking $H = 7.5$ km gives $h = 10.5$ km and $(2\Omega a)^2/g h = 8.4$ for Earthlike conditions. The resulting normal modes include low frequency westward-propagating oscillations traditionally called “Rossby-Haurwitz waves.”

(b) Bounded atmospheres

If a top exists at $x = x_T$, the upper boundary condition for normal modes is fundamentally different. As LBK point out, “there are an infinite number of h 's for which [Eq. (3)] has nontrivial solutions ... These constitute the free oscillations of the atmosphere; they include Rossby-Haurwitz waves. In an infinite atmosphere these are all associated with a single h ... [but] bounded models will have other Rossby-Haurwitz waves associated with the spurious h 's.” This can lead to problems in numerical atmospheric models.

LBK work out the details by solving Eq. (3) with a nonzero solar heating and looking for resonances. This technique will reliably get normal mode oscillations (e.g. Covey and Schubert 1982) but it's simpler to stay with the unforced problem, and impose upon Eq. (4) the lower boundary condition (5) together with a new upper boundary condition. Here I follow LBK, assuming that the pressure-coordinate vertical velocity $w^* \equiv dz^*/dt$ vanishes at $x = x_T$. Physically this assumption corresponds to a “free surface” for which $dp/dt = 0$; it was applied at $p = 0$ in the early GCMs mentioned above (Leith 1965, Hunt and Manabe 1968). Although it is not a rigid lid, this boundary introduces spurious normal modes that don't exist in a more realistic, unbounded atmosphere. For example, the equations describing gravity waves in the simplest Boussinesq approximation have no unforced solutions satisfying either the radiation condition or boundedness as $z \rightarrow \infty$, but they have an infinite number of unforced solutions satisfying $dp/dt = 0$ at finite z (Lindzen 2005, Chapter 8).

Spurious normal modes also appear in the current problem. Again the thermodynamic energy equation simplifies in the absence of forcing, so the upper boundary condition is just $w^* \propto \partial\Phi/\partial z^* \propto \partial(Ge^{x/2})/\partial x = 0$. Substituting in the functional form of $G(x)$ from Eq. (4) and the value of A from Eq. (5), it follows that the expression

$$\frac{2 e^{x_T/2} \left((2\kappa + 4\mu^2 - 1) \sinh(\mu x_T) + 4\kappa\mu \cosh(\mu x_T) \right)}{-4\kappa + 4\mu + 2}$$

must vanish. The exponential factor in the numerator is never zero, and the denominator is also nonzero because μ is either pure imaginary, or real and by definition positive (so $\mu \neq \kappa - \frac{1}{2}$ for thermodynamically valid values of κ , which must always be $< 2/5$). Thus the result of imposing the upper and lower boundary conditions is a simple equation relating μ to κ and x_T :

$$(2\kappa + 4\mu^2 - 1) \sinh(\mu x_T) + 4\kappa\mu \cosh(\mu x_T) = 0$$

(*7*)

In a bounded atmosphere, μ can be either real or imaginary. The physical meaning of imaginary μ is that waves are propagating vertically, and reflection at the top of the model can produce a resonant standing wave. In this case it is convenient to set $\mu = i|\mu|$ so that at $\sinh(\mu x_T) = i \sin(|\mu| x_T)$ and $\cosh(\mu x_T) = \cos(|\mu| x_T)$. Dividing by i , Eq. (7) then becomes

$$(-4 \operatorname{Im}\mu^2 + 2\kappa - 1) \sin(\operatorname{Im}\mu x_T) + 4 \operatorname{Im}\mu \kappa \cos(\operatorname{Im}\mu x_T) = 0$$

(*8*)

I separately solve Eq. (7) for real μ and Eq. (8) for imaginary μ . In either case the right-hand side is an odd function, so no information is lost by continuing to define μ as the positive (or positive-imaginary) square root of μ^2 . Setting $\kappa = 2/7$ and solving Eqs. (7)-(8) gives a relationship between the top height x_T and the eigenvalue μ . The result is shown in the diagram below: provided that $x_T > 8/3$, there is one real μ (blue curve) and an infinite number of imaginary μ 's (orange curves) for each choice of x_T . This can be checked against LBK's figures for model tops at 200 and 10 mb; corresponding x_T values are marked by the two horizontal black dashed lines (the vertical red dashed lines will be discussed in the next section).

In the diagram, as $\mu \rightarrow 0$ the blue line merges with the lowest orange line and both approach $x_T = 8/3$. Therefore, if the top is low enough, the one solution with real μ cannot exist. In effect it is replaced by the lowest-order solution with imaginary μ . This situation occurs, for example, when the model top is at 200 mb (lower dashed line). For this case LBK find a number of gross qualitative differences between the bounded- and unbounded-atmosphere models. Fortunately, modern climate models place their tops much higher, at or above the 10 mb pressure level.

For the model top at 10 mb (upper dashed line) LBK find that "the first free oscillation in the bounded models occurs at $h \approx 10$ km [$\mu \approx 0.2$ in the figure], which is quite near the correct value." As noted above, the correct value for an unbounded atmosphere is $\mu = \frac{1}{2} - \kappa = 0.214$. This corresponds to horizontally propagating acoustic waves that decay exponentially in the vertical, e.g. the so-called Lamb wave that has been observed with a period of 5 days. But imaginary- μ solutions appear nearby, and the bounded continuous model "exhibits spurious free oscillations for $h = 2.65, 0.98, 0.37$ [sic], ... km, etc." These h -values agree with the diagram's μ -values except for 0.37 km, which should actually be 0.47 km ("0.37" in LBK's text is a typo, as can be seen by inspecting their Fig. 4).

What happens as $x_T \rightarrow \infty$? Physically we should get back to the unbounded-atmosphere case, with just one normal-mode oscillation corresponding to a vertically evanescent wave, i.e. the vertical wavenumber μ should be real and negative. But mathematically we are retaining a boundary condition that allows imaginary as well as real values of μ . As noted above, early GCMs applied this boundary condition at $p = 0$. Although the mathematics is ambiguous (with no defined limit to Eq. (8) as $x_T \rightarrow \infty$) the imaginary μ 's show no sign of disappearing from the figure above as x_T is increased -- and as LBK point out, a top at $p = 0$ "as a result of inevitable finite-difference errors ... is equivalent to having the top at some small, finite p ."

Thus imaginary values of μ and the corresponding spurious h 's can cause problems for numerical simulations of the tides. As noted above, resonance will occur if any of the spurious h 's matches an h

that arises when thermal forcing is applied. A brief discussion of nonzero forcing is therefore appropriate. As a first approximation, I consider only the unbounded atmosphere problem when forcing is nonzero.

Classical theory of forced waves

This is approached in reverse order to the unforced problem: we first solve Laplace's tidal equation (2) with σ and s specified. "Migrating" tides that follow the apparent motion of the Sun across the sky have $\sigma = -(2\pi/24 \text{ hours}) \times s$, $s \in \{1, 2, 3, \dots\}$ giving {diurnal, semidiurnal, terdiurnal, ...} harmonics. For each harmonic, solving Eq. (2) produces a set of eigenvalues h_n^s (equivalent depths) and eigenfunctions Θ_n^s (Hough functions). Only then, for each h , do we solve the vertical structure equation (3) with nonzero forcing on the right-hand side, obtaining tidal amplitude as a function of height. (As noted above, the boundary conditions on Eq. (3) are somewhat more complicated than those presented for the unforced problem.) The forcing term in the vertical structure equation for h_n^s comes from projecting solar heating onto the Hough function $\Theta_n^s(\phi)$.

Obviously the diurnal harmonic dominates the day-to-night cycle of solar heating, but the semidiurnal harmonic is also appreciable. For example, a rectified sine wave -- at night, zero amplitude; by day, proportional to the cosine of the solar zenith angle at the Equator -- has semidiurnal amplitude a bit less than half (42%) its diurnal amplitude.

Results of the forced problem are discussed by Lindzen (2005, Chapter 9) and Chapman and Lindzen (1970) as well as compactly summarized by Forbes (1995, Table 1 and Figs. 5-7). These results agree fairly well with observations of surface-pressure tides without needing to "tune" the background atmospheric state. Most of the forcing comes from ozone absorption of solar UV around the stratopause (~30-70 km altitude) because the right-hand side in Eq. (3) is proportional to heating *per unit mass*, and the higher the energy absorption occurs, the greater the response at all levels. For the diurnal harmonic, solar heating projects mainly onto Hough functions $\Theta_{-2}^1(\phi)$ and $\Theta_1^1(\phi)$ with corresponding equivalent depths $h_{-2}^1 = -12.2703 \text{ km}$ and $h_1^1 = 0.6909 \text{ km}$ respectively. For the semidiurnal harmonic, the corresponding eigenfunctions and eigenvalues are $\Theta_2^2(\phi)$, $\Theta_4^2(\phi)$ and $\Theta_6^2(\phi)$ with $h_2^2 = 7.8519 \text{ km}$, $h_4^2 = 2.1098 \text{ km}$ and $h_6^2 = 0.9565 \text{ km}$ respectively. Associated μ values are

forcedMuList =

$$\sqrt{\frac{1}{4} - \frac{(2/7)(7.5 \text{ km})}{h}} \quad / . \text{ h} \rightarrow \{-12.2703, 0.6909, 7.8519, 2.1098, 0.9565\} \text{ km}$$

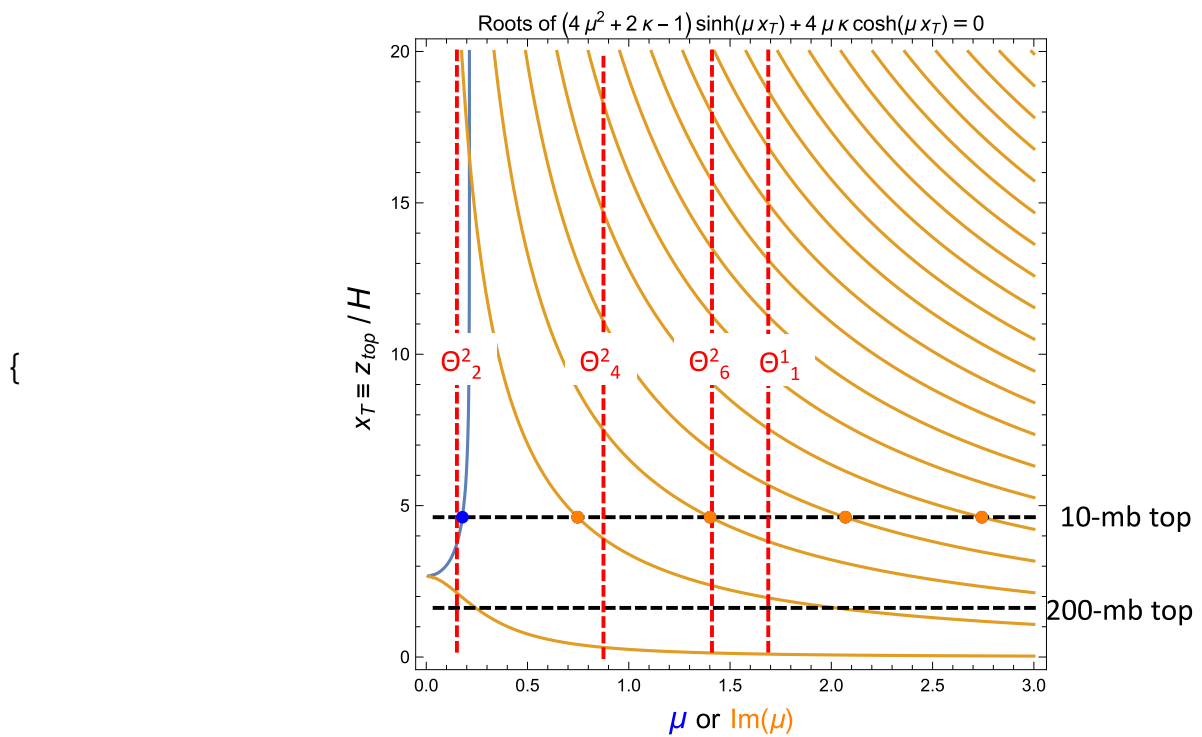
{0.651642, 0. + 1.68865 i, 0. + 0.151358 i, 0. + 0.875025 i, 0. + 1.41078 i}

Thus the first diurnally forced mode $\Theta_{-2}^1(\phi)$, with real μ , suffers vertical trapping with an e -folding depth $(\mu_{-2}^1)^{-1} \approx (0.65)^{-1}$ scale heights or 12 km, while the second diurnally forced mode $\Theta_1^1(\phi)$ propagates vertically with a wavelength no greater than the depth of ozone forcing, leading to destructive interference: $2\pi(\text{Im } \mu_1^1)^{-1} \approx 2\pi(1.69)^{-1}$ scale heights $\approx 28 \text{ km}$. Consequently, very little of the diurnal harmonic response to ozone heating reaches the surface. Instead, the diurnal surface-pressure tide is mostly generated by forcing near the surface -- particularly latent heat release and water vapor absorption of solar near-IR -- where atmospheric heating per unit mass is relatively small. In contrast, all three of the leading semidiurnally forced modes $\Theta_2^2(\phi)$, $\Theta_4^2(\phi)$ and $\Theta_6^2(\phi)$ propagate vertically, and the wavelength of the first mode is very long: $2\pi(\text{Im } \mu_2^2)^{-1} \approx 2\pi(0.15)^{-1}$ scale heights $\approx 300 \text{ km}$. The semidiurnal harmonic is mainly (~2/3) a response to ozone heating and dominates the surface-pressure tide, with nearly twice

the amplitude of the diurnal harmonic. Within the middle atmosphere and lower thermosphere, however, the diurnal harmonic generally dominates.

Forcing at resonance?

LBK point out that if “for some σ and s the resulting h_n is equal to that for free oscillations, then we will obtain an infinite response.” This can occur if a model top happens to be placed to make a spurious-resonance wavenumber $\text{Im}(\mu)$ coincide with one of the prominent eigenvalues that arise from solar heating. To see where this happens, include the solar-forced $\text{Im}(\mu)$ values listed above in the diagram:



The red dashed vertical lines are associated (from left to right) with solar-forced Hough modes $\Theta_2^2(\phi)$, $\Theta_4^2(\phi)$, $\Theta_6^2(\phi)$ and $\Theta_1^1(\phi)$. Forcing at resonance occurs for a particular value of x_T if the associated horizontal line intersects both a orange curve and one of the vertical lines. This happens once in the diagram above: a model top placed at 10 mb (~ 30 km altitude) is close to matching the vertical wavelength from semidiurnal forcing of the third meridionally symmetric Hough mode $\Theta_6^2(\phi)$: 33.4 km for an isothermal 256 K background atmosphere. But before jumping to conclusions, one must examine the actual top boundary conditions in modern climate models. These are not as simple as the $dp/dt = 0$ condition applied to the early GCMs.

According to online documentation for the Climate Model Intercomparison Project (<http://compare.es-doc.org>), top boundary conditions in modern GCMs involve either a sponge-layer treatment or a radiation condition. The actual situation is more complicated. For example, the online documentation says that the model NorESM1-M uses a radiation condition, but this model's original documentation says it closely follows CCSM4/CAM4 (Bentsen et al. 2013) and the documentation for CAM4 says "diffusion near the model top is used as a simple sponge to absorb vertically propagating planetary wave energy" (Neale et al. 2010). Similarly, the online documentation says the GISS model family uses a radiation condition, but the original documentation says it employs Rayleigh friction at the top (Schmidt et al. 2014). Models can, of course, use a combination of sponge layer and radiation boundary condition. Adding to the complication, the top itself is placed at "infinity" ($p = 0$) in about half of modern GCMs and at finite altitude (from roughly 40 to 150 km) in the other half, though some of the "infinite domain" models keep thermodynamic variables -- including solar heating -- up to only 30 km (Covey et al. 2014, Table 1).

In practice, further progress on the issue of spurious wave reflection requires a focus on just one GCM family, probably CCSM4/CAM4 including its vertically extended version WACCM4 (Marsh et al. 2013). This report will serve as a theoretical foundation for such future work.

Acknowledgments

Dick Lindzen's and Mike MacCracken's comments substantially enhanced this report. Work was performed under auspices of the DOE Office of Science at the Lawrence Livermore National Laboratory under Contract DE-AC52-07NA27344.

References

- M. Bentsen and Coauthors, 2013: The Norwegian Earth System Model, NorESM1-M -- Part 1: Description and basic evaluation of the physical climate. *Geoscientific Model Development* 6, 687-720
- S. Chapman and R. S. Lindzen, 1970: *Atmospheric Tides: Thermal and Gravitational*. Gordon and Breach Science Publishers, 200 pp.
- C. Covey and G. Schubert, 1982: Planetary-scale waves in the Venus atmosphere. *Journal of the Atmospheric Sciences* 39, 2397-2413
- C. Covey, A. Dai, D. Marsh and R. S. Lindzen, 2011: The surface-pressure signature of atmospheric tides in modern climate models. *Journal of the Atmospheric Sciences* 68, 495-514
- C. Covey, A. Dai, R. S. Lindzen and D. Marsh, 2014: Atmospheric tides in the latest generation of climate models. *Journal of the Atmospheric Sciences* 71, 1905-1913
- J. M. Forbes, 1995: Tides and planetary waves, in *The Upper Mesosphere and Lower Thermosphere: A Review of Experiment and Theory*. Geophysical Monograph No. 87, American Geophysical Union, pp. 67-87
- K. Hamilton, S. C. Ryan and W. Ohfuchi, 2008: Topographic effects on the solar semidiurnal surface tide simulated in a very fine resolution general circulation model. *Journal of Geophysical Research* 113, D17114
- J. W. Hardy, 1968: *Tides in a Numerical Model of the Atmosphere*. Lawrence Livermore National Laboratory report UCRL-50368, 49 pp. (PDF copy available on request to the author of this report)
- J. R. Holton, 1975: *The Dynamical Meteorology of the Stratosphere and Mesosphere*. Meteorological Monographs Vol. 15, No. 37, American Meteorological Society, 216 pp.

- B. G. Hunt and S. Manabe, 1968: An investigation of thermal tidal oscillations in the Earth's atmosphere using a general circulation model. *Monthly Weather Review* 96, 753-766
- C. E. Leith, 1965: Numerical simulation of the Earth's atmosphere, in *Methods in Computational Physics, Vol. 4: Applications in Hydrodynamics*. Academic Press, pp. 1-28
- R. S. Lindzen, E. S. Batten and J.-W. Kim, 1968: Oscillations in atmospheres with tops. *Monthly Weather Review* 96, 133-140
- R. S. Lindzen, 2005: *Dynamics in Atmospheric Physics*. Cambridge University Press paperback edition, 324 pp. (PDF updates available on request to either Lindzen or the author of this report)
- M. S. Longuet-Higgins, 1968: The eigenfunctions of Laplace's tidal equation on a sphere. *Philosophical Transactions of the Royal Society of London A262*, 511-607
- R. B. Neale and Coauthors, 2010: *Description of the NCAR Community Atmosphere Model (CAM 4.0)*. National Center for Atmospheric Research Technical Note 485+STR (http://www.cesm.ucar.edu/models/ccsm4.0/cam/docs/description/cam4_desc.pdf)
- G. A. Schmidt and Coauthors, 2014: Configuration and assessment of the GISS ModelE2 contributions to the CMIP5 archive. *Journal of Advances in Modeling Earth Systems* 6, 141-184
- F. Zwiers and K. Hamilton, 1986: Simulation of solar tides in the Canadian Climate Center general circulation model. *Journal of Geophysical Research* 93, 11877-11896